JOURNAL OF AIRCRAFT
Vol. 42, No. 2, March–April 2005

Analysis of Bending Vibration of Rectangular Plates Using Two-Dimensional Plate Modes

Gang Wang* and Norman M. Wereley†
University of Maryland, College Park, Maryland 20742
and
Der-Chen Chang‡
Georgetown University, Washington, DC 20057

A higher order assumed modes (Ritz) method is developed for rectangular plate analysis using two-dimensional plate mode shape functions. These two-dimensional plate mode shape functions were determined using the extended Kantorovich–Krylov method. The rectangular plate is assumed isotropic and uniform, and has each edge of its span (root and tip) clamped and remaining edges free (clamped–free–clamped–free boundary conditions). Natural frequencies, mode shape functions, and frequency responses of the plate were calculated and compared to the results of traditional analysis using one-dimensional beam modes to approximate plate modes in both *x* and *y* directions. The updated two-dimensional plate mode shape functions substantially reduce the computational cost compared to the case of using one-dimensional beam mode shape functions. Fewer modes are needed in the proposed method to yield the same accuracy. Experiments were conducted to validate our predictions and the data agree with our predictions.

Nomenclature

a	=	length of plate in x direction
b	=	length of plate in y direction
E	=	Young's modulus of plate material
h	=	plate thickness
m, n	=	number of half-wavelengths for mode shapes
W	=	mode shape function of w
w	=	displacement in transverse bending direction
X	=	separable component of a mode shape function for W in x direction
Y	=	separable component of a mode shape function for W in y direction
α	=	ratio of length in x and y directions
ζ	=	nondimensional length in x direction
η	=	nondimensional length in x direction
ν	=	Poisson's ratio of plate
ρ	=	density of plate
Ω	=	nondimensional frequency
Ω_x	=	nondimensional frequency solution in x direction
Ω_y	=	nondimensional frequency solution in y direction
ω	=	excitation frequency

Introduction

THE transverse bending vibration of thin rectangular plates under the Kirchhoff hypothesis is considered in this paper. Exact solutions exist only for Levy-type plates, in which at least two opposite edges are simply supported.[1−3] The displacement can be determined using separation of variables, which reduces the plate problem to a beamlike one-dimensional problem. For other plate boundary conditions, the natural frequencies were calculated by the assumed modes (Ritz) method.[1,4] Leissa[1] reviewed natural frequency results for plates with a wide range of boundary conditions. One-dimensional beam mode shape functions have been used to approximate the two-dimensional plate modes by approximating them as a product of two separable beam mode shapes in x and y directions. A linear combination of these assumed plate modes was then employed to represent actual plate vibration modes. These beam mode shape functions can easily satisfy the geometric boundary conditions along the plate edges. The unknown coefficients for each assumed mode minimize the total energy and yield the approximate natural frequencies. A large size eigenvalue problem must be used to calculate the natural frequencies because many assumed modes are needed to improve frequency prediction accuracy. In some cases, an assumed mode can satisfy both geometric and force boundary conditions, which leads to the Galerkin method. This approach can provide us with an exact solution because the assumed mode is identical to the actual vibration mode. However, it is very difficult to find such assumed modes that satisfy both geometric and force boundary conditions. Therefore, our efforts focus on how to improve our assumed modes.

The Kantorovich–Krylov method[5] is a variational method that can reduce the partial differential equations (PDEs) to ordinary differential equations (ODEs). Similar to the assumed modes method, the Kantorovich–Krylov method tries to find the function minimizing the integral of total potential energy instead of solving the boundary-value problem of PDEs. As stated by Kantorovich and Krylov, "[t]he advantage of this method, apart from its greater accuracy, consists in that only part of the expression giving the solutions is chosen a priori; part of the functions being determined in accordance with the character of the problem." This is a one-step process with no iteration involved, which is called the traditional Kantorovich–Krylov method. Kerr[6] was the first to propose the extended Kantorovich–Krylov method and applied it to the torsion problem of a beam with rectangular cross section, in which single-term separable displacement approximation generated good results. Basically we assume a separable representation for the solution function. Iteratively, we solve for the separable components, which yields a convergent sequence of results. This approach is called the extended

Presented as Paper 2003-1774 at the AIAA/ASME/ASCE/AHS 44th Structures, Structural Dynamics, and Materials Conference, Norfolk, VA, 7–10 April 2003; received 1 August 2003; revision received 15 December 2003; accepted for publication 19 December 2003.

*Research Associate, Smart Structures Laboratory, Alfred Gessow Rotorcraft Center, Department of Aerospace Engineering; gwang@eng.umd.edu. Member AIAA.

†Associate Professor of Aerospace Engineering, Smart Structures Laboratory, Alfred Gessow Rotorcraft Center, Department of Aerospace Engineering; wereley@eng.umd.edu. Associate Fellow AIAA.

‡Professor and Director, Mathematical Sciences Center, Department of Mathematics; chang@georgetown.edu.

Kantorovich–Krylov method. Subsequently, Kerr and Alexander[7] applied the extended Kantorovich–Krylov method to the stress analysis of a clamped rectangular plate, and the membrane vibration and plate bending stability problems were solved as shown in Ref. 8. Because the extended Kantorovich–Krylov method is a semi-analytical method and some parameters must be determined numerically, the method did not receive widespread acceptance.

However, improvements in computational power have resulted in a resurgence of interest in the extended Kantorovich method during the past decade.[9–13] Cortinez and Laura[9] studied bending vibration of stepped rectangular plates using the traditional Kantorovich–Krylov method. Bhat et al.[10] solved for plate bending mode shapes for boundary condition combinations of simply supported and clamped cases using the extended Kantorovich–Krylov method. Rajalingham et al.[11,12] applied the same method to the rectangular plate bending vibration problem. All these successes prove that the extended Kantorovich–Krylov method is a universal and powerful mathematical tool for PDEs. However, all of these results were only validated analytically with no comparisons to experimental data. We applied the extended Kantorovich–Krylov method to in-plane vibration problems of rectangular plates.[13] The mathematical representation of this approach and application for in-plane plate vibration are presented by Chang et al.[14] We have also investigated the application of the extended Kantorovich–Krylov method to biharmonic PDEs of which the out-of-plane plate bending vibration is a notable example.[15] In Ref. 15 we presented a detailed convergence proof of the method. The basis of this proof is that the separable variable solutions are the projections of the exact solutions and the solution sequence converges and reaches the minimum in the sense of an $L2$ norm.

In this paper, we applied the extended Kantorovich–Krylov method to rectangular plate bending vibration and validated our results by experiment and the assumed modes method, where plate modes were approximated by beam modes in both x and y directions. We consider a rectangular plate with clamped–free–clamped–free (CFCF) boundary conditions, as shown in Fig. 1. The plate is 304.8 mm (12 in.) long, 254 mm (10 in.) wide, and 1.52 mm (0.05975 in.) thick and is made of aluminum. The two-dimensional plate mode shape functions were calculated using the extended Kantorovich–Krylov method and were employed in the assumed modes method for plate bending analysis. The two-dimensional assumed mode results were compared to plate modes approximated as the product of one-dimensional beam mode shape functions in both x and y directions. Natural frequency, mode shape functions, and frequency response were validated by the experimental data and the results agree well. Fewer modes are needed in the assumed modes method when using two-dimensional plate mode shape functions determined by the extended Kantorovich–Krylov method, and the same accuracy is achieved compared to the case of using one-dimensional beam modes. This leads to a higher order assumed modes method for plate bending analysis.

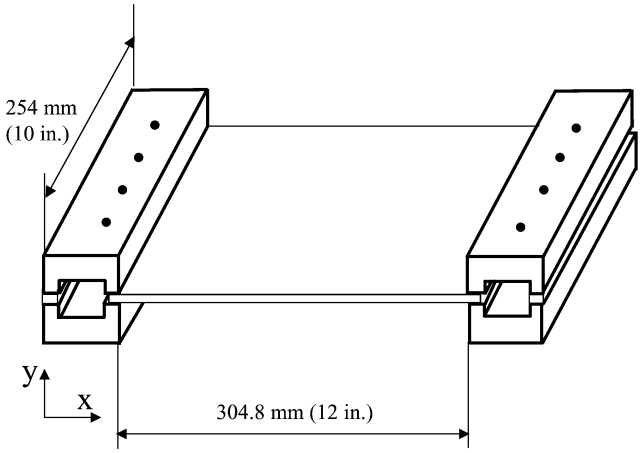

Fig. 1 Plate under CFCF boundary conditions.

Governing Equations

A uniform rectangular thin plate with Kirchhoff hypothesis is considered, and the potential energy is

$$U = \frac{1}{2}\int_0^a \int_0^b D\left[\left(\frac{\partial^2 w}{\partial x^2}\right)^2 + \left(\frac{\partial^2 w}{\partial y^2}\right)^2 + 2\nu\frac{\partial^2 w}{\partial x^2}\frac{\partial^2 w}{\partial y^2} + 2(1-\nu)\left(\frac{\partial^2 w}{\partial x\,\partial y}\right)^2\right] \mathrm{d}x\,\mathrm{d}y \tag{1}$$

The kinetic energy is

$$T = \frac{1}{2}\int_0^a \int_0^b \rho h\left(\frac{\partial w}{\partial t}\right)^2 \mathrm{d}x\,\mathrm{d}y \tag{2}$$

where the plate bending flexural stiffness is

$$D = \frac{Eh^3}{12(1-\nu^2)}$$

Applying the Hamiltonian principle, the governing equation is[2,16]

$$D\left(\frac{\partial^4 w}{\partial x^4} + 2\frac{\partial^2 w}{\partial x^2 y^2} + \frac{\partial^4 w}{\partial y^4}\right) + \rho h\frac{\partial^2 w}{\partial t^2} = 0 \tag{3}$$

and associated boundary conditions along two edges in the x direction (i.e., $x = 0, a$) are

$$M_x = D\left(\frac{\partial^2 w}{\partial x^2} + \nu\frac{\partial^2 w}{\partial y^2}\right) = 0 \quad \text{or} \quad \frac{\partial w}{\partial x} = 0$$

$$V_x = D\left[\frac{\partial^3 w}{\partial x^3} + (2-\nu)\frac{\partial^3 w}{\partial x\,\partial y^2}\right] = 0 \quad \text{or} \quad w = 0$$

The boundary conditions along two edges in the y direction (i.e., $y = 0, b$) are

$$M_y = D\left(\frac{\partial^2 w}{\partial y^2} + \nu\frac{\partial^2 w}{\partial x^2}\right) = 0 \quad \text{or} \quad \frac{\partial w}{\partial y} = 0$$

$$V_x = D\left[\frac{\partial^3 w}{\partial y^3} + (2-\nu)\frac{\partial^3 w}{\partial x^2\,\partial y}\right] = 0 \quad \text{or} \quad w = 0$$

Also, the corner conditions are

$$\frac{\partial^2 w}{\partial x\,\partial y} = 0$$

To solve the preceding equations, we assume that a time response $w(x, y, t)$ is the product of a harmonic time response and a displacement mode shape function $W(x, y)$ so that

$$w(x, y, t) = W(x, y)e^{j\omega t} \tag{4}$$

and we assume that the mode shape function $W(x, y)$ is separable:

$$W(x, y) = X(x)Y(y) \tag{5}$$

Substituting Eqs. (4) and (5) into Eq. (3) yields

$$\frac{\mathrm{d}^4 X}{\mathrm{d}x^4}Y + 2\frac{\mathrm{d}^2 X}{\mathrm{d}x^2}\frac{\mathrm{d}^2 Y}{\mathrm{d}y^2} + X\frac{\mathrm{d}^4 Y}{\mathrm{d}y^4} - \frac{\rho h\omega^2}{D}XY = 0 \tag{6}$$

Obviously, the separable solution for $W(x, y)$ consisting of the functions X and Y exists only if either of the following conditions holds:

$$\frac{\mathrm{d}^2 X}{\mathrm{d}x^2} = \gamma_1 X, \qquad \frac{\mathrm{d}^2 Y}{\mathrm{d}y^2} = \gamma_2 Y$$

where γ_1 and γ_2 are constants. These mathematical expressions imply that opposite edges have to be simply supported boundaries to

satisfy the conditions of separable solutions. Thus, only Levy-type plates have closed-form separable solutions.[1–3] For other boundary conditions, separable solutions for plate mode shape functions cannot be obtained. Thus, the separable representation of the transverse displacement mode shapes is only an approximation. Therefore, we resort to the extended Kantorovich–Krylov method to find a higher order solution of the separable plate bending modes.

Extended Kantorovich–Krylov Method

In this section, we will show the application of the extended Kantorovich–Krylov method for plate bending vibration. Because this approach has been presented before,[10–12] we outline the approach and present the key results. As mentioned earlier, we seek the functions that minimize the integral of total plate bending energy instead of solving a boundary-value problem, as shown in Eq. (3). We substitute Eqs. (4) and (5) into Eqs. (1) and (2) and take its variation. Finally, the corresponding nondimensional variational expression of total energy of a plate is

$$\delta U = \int_0^1\int_0^1 \left(\frac{\partial^4 W}{\partial\zeta^4} + 2\alpha^2\frac{\partial^4 W}{\partial\zeta^2\partial\eta^2} + \alpha^4\frac{\partial^4 W}{\partial\eta^4} + \Omega^2 W\right)\delta W\,\mathrm{d}\zeta\,\mathrm{d}\eta + \int_0^1\left[M_\zeta\delta\left(\frac{\partial W}{\partial\zeta}\right)\right]_0^1\mathrm{d}\eta + \int_0^1\left[M_\eta\delta\left(\frac{\partial W}{\partial\eta}\right)\right]_0^1\mathrm{d}\zeta - \int_0^1[V_\zeta\delta W]_0^1\,\mathrm{d}\eta - \int_0^1[V_\eta\delta W]_0^1\,\mathrm{d}\zeta - \left[\left[2(1-\mu)\alpha^2\frac{\partial^2 W}{\partial\zeta\,\partial\eta}\delta W\right]_0^1\right]_0^1 = 0 \tag{7}$$

Here we define some nondimensional parameters. The nondimensional lengths in the x and y directions are

$$\zeta = x/a, \qquad \eta = y/b$$

The aspect ratios of plate and nondimensional frequency are

$$\alpha = a/b, \qquad \Omega^2 = \omega^2(\rho h a^4/D)$$

The nondimensional resultant shear forces and moments are

$$V_\zeta = \frac{\partial^3 w}{\partial\zeta^3} + \alpha^2(2-\nu)\frac{\partial^3 w}{\partial\zeta\,\partial\eta^2}$$

$$V_\eta = \alpha^4\frac{\partial^3 w}{\partial\eta^3} + \alpha^2(2-\nu)\frac{\partial^3 w}{\partial\zeta^2\partial\eta}$$

$$M_\zeta = \frac{\partial^2 w}{\partial\zeta^2} + \nu\alpha^2\frac{\partial^2 w}{\partial\eta^2}, \qquad M_\eta = \alpha^4\frac{\partial^2 w}{\partial\eta^2} + \nu\alpha^2\frac{\partial^2 w}{\partial\zeta^2}$$

The separable solution of bending mode shape function, W_{mn}, is assumed to be separable as follows:

$$W_{mn}(\zeta,\eta) = X_m(\zeta)Y_n(\eta) \tag{8}$$

Now the question is how to determine X_m and Y_n.

Determination of $X_m(\zeta)$

If we assume Y_n is prescribed a priori, then

$$\delta W_{mn}(\zeta,\eta) = Y_n(\eta)\delta X_m(\zeta) \tag{9}$$

Substituting Eqs. (8) and (9) into Eq. (7) and integrating along the η direction yields an ODE for $X_m(\zeta)$:

$$\frac{\mathrm{d}^4 X_m}{\mathrm{d}\zeta^4} + 2\beta_x\frac{\mathrm{d}^2 X_m}{\mathrm{d}\zeta^2} + \gamma_x X_m = 0 \tag{10}$$

where β_x is a constant and γ_x is a function of unknown parameter Ω. The expressions for these two parameters are

$$\beta_x = \frac{\int_0^1\alpha^2 Y_n''Y_n\,\mathrm{d}\eta + \alpha^2(\nu-1)[Y_n'Y_n]_0^1}{\int_0^1 Y_n^2\,\mathrm{d}\eta}$$

$$\gamma_x = \frac{\int_0^1\alpha^4 Y_n''''Y_n\,\mathrm{d}\eta + \alpha^4\left([Y_n''Y)n']_0^1 - [Y_n'''Y_n]_0^1\right)}{\int_0^1 Y_n^2\,\mathrm{d}\eta} - \Omega^2$$

where, in this case,

$$()' = \frac{\mathrm{d}}{\mathrm{d}\eta}()$$

The solution of Eq. (10) is an expansion of four waves:

$$X_m = c_1\sin(p_x\zeta) + c_2\cos(p_x\zeta) + c_3\sinh(q_x\zeta) + c_4\cosh(q_x\zeta) \tag{11}$$

where

$$p_x = \left|\sqrt{-\beta_x - \sqrt{\beta_x^2 - 4\gamma_x}}\right|, \qquad q_x = \left|\sqrt{-\beta_x + \sqrt{\beta_x^2 - 4\gamma_x}}\right|$$

and where p_x and q_x are wave numbers, which are functions of Ω. The wave coefficients c_1, c_2, c_3, and c_4 are determined using the boundary condition at the two edges, $\zeta = 0$ and $\zeta = 1$. The possible boundary conditions on these two edges are: 1) clamped edge,

$$X_m = 0, \qquad \frac{\mathrm{d}X_m}{\mathrm{d}\zeta} = 0$$

2) simply supported edge,

$$X_m = 0, \qquad \frac{\mathrm{d}^2 X_m}{\mathrm{d}\zeta^2} = 0$$

or 3) free edge,

$$\frac{\mathrm{d}^2 X_m}{\mathrm{d}\zeta^2} + e_1 X_m = 0, \qquad \frac{\mathrm{d}^3 X_m}{\mathrm{d}\zeta^3} + e_2\frac{\mathrm{d}X_m}{\mathrm{d}\zeta} = 0$$

where

$$e_1 = \nu\alpha^2\frac{\int_0^1 Y_n''Y_n\,\mathrm{d}\eta}{\int_0^1 Y_n^2\,\mathrm{d}\eta}$$

$$e_2 = \alpha^2(2-\nu)\frac{\int_0^1 Y_n''Y_n\,\mathrm{d}\eta}{\int_0^1 Y_n^2\,\mathrm{d}\eta} - 2\alpha^2(1-\nu)\frac{[Y_n'Y_n]_0^1}{\int_0^1 Y_n^2\,\mathrm{d}\eta}$$

The next step is to determine the wave coefficients, c_1, c_2, c_3, and c_4. For example, for the case in which a plate is clamped at $\zeta = 0$ and free at $\zeta = 1$,

$$\begin{bmatrix} 0 & 1 & 0 & 1 \\ p_x & 0 & q_x & 0 \\ f_1\sin(p_x) & f_1\cos(p_x) & f_2\sinh(q_x) & f_2\cosh(q_x) \\ f_3\cos(p_x) & f_4\sin(p_x) & f_5\cosh(q_x) & f_5\sinh(q_x) \end{bmatrix}\begin{bmatrix} c_1 \\ c_2 \\ c_3 \\ c_4 \end{bmatrix} = 0 \tag{12}$$

where

$$f_1 = -p_x^2 + e_1, \qquad f_2 = q_x^2 + e_1, \qquad f_3 = -p_x^3 + e_2 p_x$$

$$f_4 = p_x^3 - e_2 p_x, \qquad f_5 = q_x^3 + e_2 q_x$$

The nontrivial solutions of the wave coefficients lead to an equation for the frequency Ω only. Equation (12) is solved to obtain Ω_{xm} and the coefficients in mode shape function X_m are determined.

Determination of $Y_n(\eta)$

If we assume that X_m is prescribed a priori, then

$$\delta W_{mn}(\zeta, \eta) = X_m(\zeta)\delta Y_n(\eta) \tag{13}$$

We substitute the preceding equation into Eq. (7) and integrate along the ζ direction, which yields an ODE in terms of Y_n:

$$\frac{\mathrm{d}^4 Y_n}{\mathrm{d}\eta^4} + 2\beta_y \frac{\mathrm{d}^2 Y_n}{\mathrm{d}\eta^2} + \gamma_y Y_n = 0 \tag{14}$$

where β_y is a constant and γ_y is a function of unknown parameter Ω. The expressions for these two parameters are

$$\beta_y = \frac{\int_0^1 \alpha^2 X_m'' X_m \,\mathrm{d}\zeta + \alpha^2(\nu-1)[X_m' X_m]_0^1}{\alpha^4 \int_0^1 X_m^2 \,\mathrm{d}\zeta}$$

$$\gamma_y = \frac{\int_0^1 X_m'''' X_m \,\mathrm{d}\zeta + \left([X_m'' X_m']_0^1 - [X_m''' X_m]_0^1\right)}{\alpha^4 \int_0^1 X_m^2 \,\mathrm{d}\zeta} - \frac{\Omega^2}{\alpha^4}$$

where

$$()' = \frac{\mathrm{d}}{\mathrm{d}\zeta}()$$

The solution of the preceding equations is an expansion of four waves:

$$Y_n = d_1 \sin(p_y\eta) + d_2 \cos(p_y\eta) + d_3 \sinh(q_y\eta) + d_4 \cosh(q_y\eta) \tag{15}$$

Similarly, the wave numbers are given by:

$$p_y = \left|\sqrt{-\beta_y - \sqrt{\beta_y^2 - 4\gamma_y}}\right|, \qquad q_y = \left|\sqrt{-\beta_y + \sqrt{\beta_y^2 - 4\gamma_y}}\right|$$

The possible boundary conditions along two edges $\eta = 0$ and $\eta = 1$ are 1) clamped edge,

$$Y_n = 0, \qquad \frac{\mathrm{d}Y_n}{\mathrm{d}\eta} = 0$$

2) simply-supported edge,

$$Y_n = 0, \qquad \frac{\mathrm{d}^2 Y_n}{\mathrm{d}\eta^2} = 0$$

or 3) free edge,

$$\frac{\mathrm{d}^2 Y_n}{\mathrm{d}\eta^2} + g_1 Y_n = 0, \qquad \frac{\mathrm{d}^3 Y_n}{\mathrm{d}\eta^3} + g_2 \frac{\mathrm{d}Y_n}{\mathrm{d}\eta} = 0$$

where

$$g_1 = \nu \frac{\int_0^1 X_m'' X_m \,\mathrm{d}\zeta}{\alpha^2 \int_0^1 X_m^2 \,\mathrm{d}\zeta}$$

$$g_2 = (2-\nu)\frac{\int_0^1 X_m'' X_m \,\mathrm{d}\zeta}{\int_0^1 Y_n^2 \,\mathrm{d}\eta} - 2(1-\nu)\frac{[X_m' X_m]_0^1}{\alpha^2 \int_0^1 X_m^2 \,\mathrm{d}\zeta}$$

By applying boundary conditions at two edges $\eta = 0, 1$, we can solve a frequency equation to obtain Ω_{yn} and determine the wave coefficients of $Y_n(\eta)$, as shown in Eq. (15).

Table 1 Parameters in mode shape functions of a rectangular plate bending vibration under CFCF boundary conditions and with aspect ratio of 1.2[a]

mn	c_1	c_2	c_3	p_1	p_2
11	−1.0178	−1	1.0178	4.73	4.73
12	−0.66723	−0.66521	0.66723	4.3184	6.4917
13	−0.34224	−0.34223	0.34224	3.8011	11.107
21	−0.99922	−1	0.99922	7.8532	7.8532
22	−0.85319	−0.8534	0.85319	7.6959	9.0179
23	−0.58047	−0.58048	0.58047	7.3351	12.636
14	−0.21751	−0.21752	0.21752	3.57	16.412
31	−1	−1	1	10.996	10.996
32	−0.92407	−0.92406	0.92407	10.917	11.814
24	−0.40667	−0.40667	0.40667	7.0557	17.35
33	−0.72414	−0.72414	0.72414	10.678	14.746
15	−0.15635	−0.15886	0.15886	3.4542	21.744
41	−1	−1	1	14.137	14.137
42	−0.95656	−0.95656	0.95656	14.093	14.733
34	−0.44212	−0.43507	0.43507	10.251	23.563
25	−0.20792	−0.30277	0.30277	6.7822	22.401

[a] $X_m = \sin[p_1(x/a)] + c_1 \cos[p_1(x/a)] + c_2 \sinh[p_2(x/a)] + c_3 \cosh[p_2(x/a)]$.

Iteration

We will repeat the aforementioned procedure in each of the ζ and η directions until convergence is achieved for the modal frequency in both x and y directions; that is, $\|\Omega_{xm} - \Omega_{yn}\| \le \epsilon$ ($\epsilon = 10^{-5}$ in our calculation). Then the modal frequency Ω_{mn} and mode shapes W_{mn} are determined. The algorithm is summarized in the following steps:

1) In the η direction, prescribe the mode shape Y_n^0 a priori, for iteration $k = 0$.

2a) Increment k, $Y_n^k = Y_n^{k-1}$.

2b) Obtain the ODEs in terms of X_m^k as shown in Eq. (10). Numerically solve for Ω_{xm}^k to result in a zero determinant. The wave coefficients in X_m^k are determined.

2c) Using mode shape function X_m^k as calculated in step 2b, obtain the ODEs in terms of Y_n^k as shown in Eq. (14). Numerically solve for Ω_{yn}^k to result in a zero determinant. The wave coefficients in Y_n^k are determined.

3) Check convergence between Ω_{xm}^k and Ω_{yn}^k. If $\|\Omega_{xm}^k - \Omega_{yn}^k\| \le \epsilon$, then we stop the iteration. The mode frequency of mode mn was determined. In our calculation, we set $\epsilon = 10^{-5}$. Otherwise, go to step 2a, $k = k + 1$.

To execute our algorithm, we assume an initial separable function in the y direction, that is, Y_n. A sensible choice is a beam bending mode shape, as shown in Ref. 17. Basically, we choose the corresponding beam mode shape functions matching the plate boundary conditions in the y direction. We analyzed a plate with CFCF boundary conditions, as shown in Fig. 1. For example, we assumed the second mode shape function in the y direction using beam mode shape functions for a beam with free–free boundary conditions. Then we plotted the results between determinant and nondimensional frequency as shown in Fig. 2. By observing the plots, we can pick one possible initial guess for the nondimensional frequency to vanish the determinant. Using an optimization scheme, we can solve for an Ω_x and determine the associated mode shape function in the x direction. Iteratively, we solve for Ω_y and determine the mode shape functions in the y direction. Finally we obtain nondimensional frequency and associated mode shape functions in both x and y directions using the preceding iteration scheme. The MatLab software package was used in our calculation. Validation of this method for plate bending vibration is presented in Tables 1 and 2 for the first 16 modes. In the preceding algorithm, we initiated the iteration from the x direction but it is equally valid to begin the algorithm in the y direction by prescribing the initial choice of X_m.

Experimental Setup

To validate our analyses, experiments were conducted. Figure 3 shows the experimental setup. A shaker was used as the excitation source, which was suspended about 381 mm (15 in.) above the plate.

The force output from the shaker was transmitted through a load cell and a rigid rod to the plate, as shown in Fig. 3. The rigid rod was bonded to the surface of plate using *M* bond and provided a good adhesion between the rod and plate. The size of the rod is about 38.1 mm (1.5 in.) long and 7.9375 mm (5/16 in.) in diameter. The load cell provided the magnitude of force input to the plate.

As shown in Fig. 3, our base is an optical table with a vibration isolation system. This isolation workstation is made by Newport Corporation. The optical table is model RS-3000 with integrated tuned damping. The top surface is 400-series ferromagnetic stainless steel with a 25.4 by 25.4 mm (1 by 1 in.) screw pattern; the diameter is 7.9375 mm (5/16 in.). An air compressor served as the air source to the isolation legs of the workstation system. The isolation system floats the table and very-low-frequency disturbances from the floor were isolated. Details are given by Fowler et al.[18]

A plate was clamped by a fixture on two parallel edges and was free on the other two edges, as shown in Fig. 3. The fixture was designed to provide clamped boundary conditions and was made of top and bottom parts. The size of top and bottom parts were the same: 381 mm (15 in.) long, 76.2 mm (3 in.) wide, and 25.4 mm (1 in.) thick. The two bottom pieces were bolted to the optical table 304.8 mm (12 in.) apart. A 330.2 by 25.4 mm (13 by 10 in.) aluminum plate specimen with a thickness of 1.52 mm (0.05975 in.) was placed atop the two bottom pieces. The clamping width was a half-inch at each clamped edge. A torque of 22.597 N · m (200 in · lbs) was applied to each of the bolts to provide uniform clamping. Figure 4 displays the details of the clamping fixture.

Table 2 Parameters in mode shape functions of a rectangular plate bending vibration under CFCF boundary condition and with aspect ratio of 1.2[a]

mn	d_1	d_2	d_3	q_1	q_2
11	0	5.6667	−0.97247	5.9605*e*−8	4.1336
12	−0.83363	2.3621	−1.0171	2.4631	4.7685
13	−0.90998	1.3878	−0.99696	5.1225	6.4879
21	0	5.6667	−0.9995	5.9006*e*−7	7.9974
22	−0.85708	3.6575	−1.0004	2.6812	8.4014
23	−0.83308	2.0886	−0.99987	5.5241	9.6129
14	−0.95901	1.1596	−1.0003	8.0428	8.9421
31	0	5.6667	−0.99999	5.4355*e*−6	11.72
32	−1.0015	4.4464	−1	2.6985	12.017
24	−0.88937	1.5344	−1	8.3742	11.427
33	−0.81327	2.7931	−1	5.7165	12.985
15	−0.97745	1.0832	−0.99998	11.098	11.75
41	0	5.6667	−1	2.5194*e*−5	15.437
42	−1.63787	4.8953	−1	2.6597	15.66
34	−0.87957	1.6052	−1	11.564	16.326
25	−0.92985	1.2948	−1	11.321	13.63

[a] $Y_n = d_1 \sin[q_1(y/b)] + d_2 \cos[q_1(y/b)] + d_3 \sinh[q_2(y/b)] + \cosh[q_2(y/b)]$.

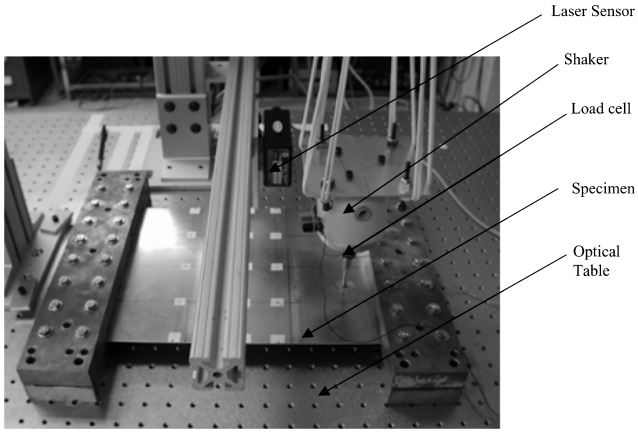

Fig. 3 Photograph of plate testing setup.

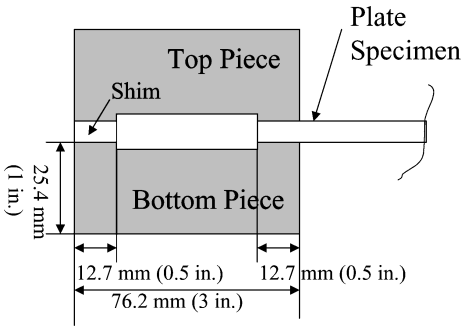

Fig. 4 Diagram of clamping fixture.

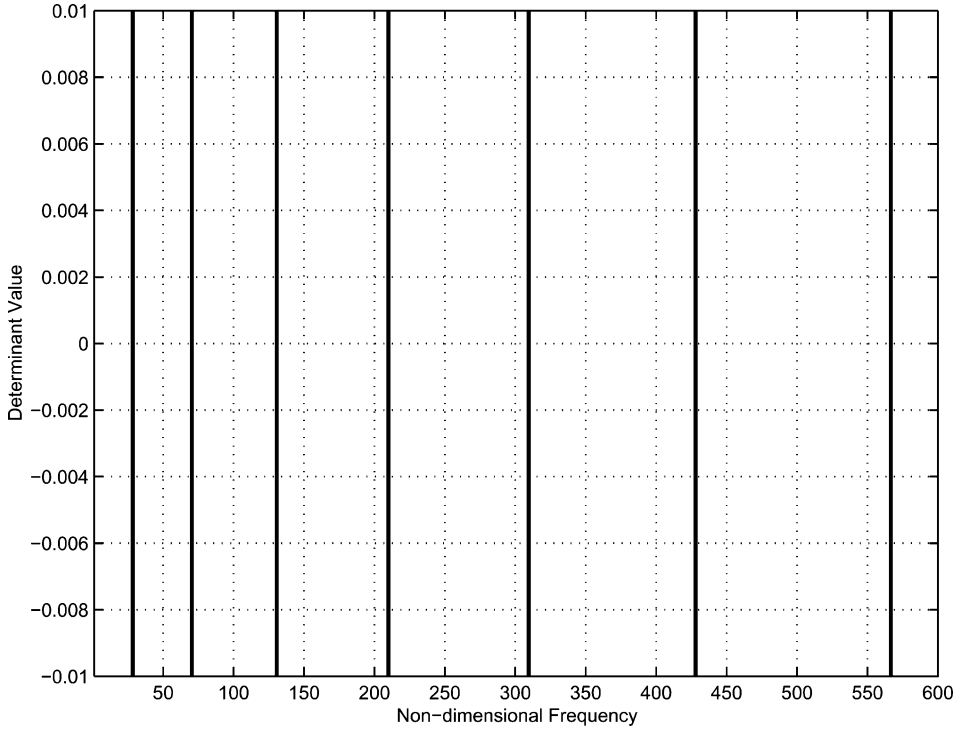

Fig. 2 Plots of determinant and nondimensional frequency assuming second mode in *y* direction for a CFCF plate.

Our specimen is an aluminum plate, which was 304.8 mm (12 in.) long, 254 mm (10 in.) wide, and 1.52 mm (0.05975 in.) thick. The aluminum plate was 6061T6 with Young's modulus $E = 68$ GPa and Poisson ratio $\nu = 0.3$. As shown in Fig. 3, a noncontact Schaevitz Distance Star laser sensor was used to measure plate displacement. We obtained a frequency response function at 15 positions on the plate. The coordinates of these measurements are listed in Table 3 for our specimen.

We chose the excitation location carefully to avoid excitation at a nodal line position of the plate; the excitation location was located at $(x, y) = (276.225, 73.025$ mm) $((10\frac{5}{8}, 2\frac{7}{8}$ in.).

A sine sweep signal was applied to the shaker with the load cell feedback to maintain the constant force magnitude for the whole frequency spectrum. We set up the control voltage in input of the load cell and the output voltage to the shaker was adjusted based on the feedback control algorithm integrated in the SigLab signal acquisition system.

Results

Based on the experimental frequency response functions at 15 locations on the plate specimen, we can extract the first seven modal frequencies, modal damping, and mode shape functions using the Star software.[19] These results were used to validate our analysis of an aluminum plate. In our analysis, the assumed modes method was employed to solve the aluminum plate vibration problem. Two analyses were developed. In analyses 1, the plate transverse displacement mode shape functions were approximated by the product of one-dimensional beam mode shapes in both x and y directions. In analysis 2, the plate mode shape functions were determined using the extended Kantorovich–Krylov method as shown in Tables 1 and 2. Finally we discuss the computational cost involved in our analyses 1 and 2 and tradeoff.

Validation

In analysis 1, the transverse displacement $w(x, y)$ was assumed to be an expansion of beam mode shape function in both x and y directions:

$$w(x, y) = \sum_i Q_i(t)\phi_m(x)\phi_n(y) \tag{16}$$

The mode shape functions ϕ_m and ϕ_n were the beam bending mode shape functions that were adapted based on the boundary conditions of the aluminum plate. The CFCF boundary conditions were considered. In the x direction, the mode shapes were the beam bending modes with clamped–clamped boundary conditions:

$$\phi_m(x) = \cosh(\beta_m x) - \cos(\beta_m x) - \lambda_m[\sinh(\beta_m x) - \sin(\beta_m x)]$$

$$\lambda_m = \frac{\cosh(\beta_m a) - \cos(\beta_m a)}{\sinh(\beta_m a) - \sin(\beta_m a)} \tag{17}$$

where β_m is determined using the characteristic equation for the fixed–fixed boundary condition of a beam,

$$\cos(\beta_m a)\cosh(\beta_m a) = 1 \tag{18}$$

where a is the length in the x direction. Along the y direction, the beam modes with free–free boundary conditions were used:

$$\phi_n(y) = \cosh(\beta_n y) + \cos(\beta_n y) - \lambda_n[\sinh(\beta_n y) + \sin(\beta_n y)]$$

$$\lambda_n = \frac{\cosh(\beta_n b) - \cos(\beta_n b)}{\sinh(\beta_n b) - \sin(\beta_n b)} \tag{19}$$

where β_n is determined using the characteristic equation for the free–free boundary condition of a beam, which is

$$\cos(\beta_n b)\cosh(\beta_n b) = 1 \tag{20}$$

We have to include as many assumed modes as possible to approximate plate modes. The simplest method is to pick up the same number of beam modes in both x and y directions. The total number of assumed plate modes i will be $m \times n$, and the modal number sequence is generated by permuting m and n. In our calculation, we use the first 5 beam modes in both x and y directions and yield a total of 25 assumed plate modes. Also, we calculated natural frequencies using a total of seven assumed plate modes, where the beam modes used in both x and y directions are intended to approximate the corresponding first seven plate modes.

Based on the extended Kantorovich–Krylov method, we determined the plate mode shape functions, as shown in Tables 1 and 2, for our particular CFCF plate. We assumed that

$$w(x, y) = \sum_i Q_i(t)X_m(x)Y_n(y) \tag{21}$$

We computed the mode shapes and modal frequencies of the first seven plate modes, which correspond to the first seven measured plate modes. The modal frequency predictions using beam and plate modes are listed in Table 4 and are compared to experimental results. For the first mode, the errors were the largest of all analyses, about 5%, this is due to the boundary condition effects. From the second to the seventh modes, the frequency prediction errors decreased in all analyses and the error in the analysis using plate mode shapes was less than that in the analyses using beam modes except for the

Table 3 Coordinates of the 15 measured locations for an aluminum plate under CFCF boundary conditions

	Coordinates[a]	
Location	x, mm	y, mm
1	76.2	250.83
2	76.2	190.5
3	75.41	127
4	74.61	64.29
5	74.61	3.175
6	152.4	250.825
7	152.4	189.71
8	152.4	127
9	152.4	61.92
10	152.4	3.175
11	190.5	250.93
12	190.5	191.29
13	191.29	127
14	190.5	63.5
15	190.5	3.175

Table 4 Bending frequency results for an aluminum plate with CFCF boundary conditions

Bending		Plate modes, $i = 7$		Beam modes, $i = 7$		Beam modes, $i = 25$	
mode no	Expt., Hz	Analysis, Hz	Error, %	Analysis, Hz	Error, %	Analysis, Hz	Error, %
1, 1	83.7	87.8	4.9	88.18	5.35	88.18	5.35
1, 2	107.3	111.01	3.45	111.54	3.95	111.28	3.71
1, 3	207.13	209.52	1.15	212.11	2.41	209.73	1.26
2, 1	233.68	241.56	3.37	243.06	4.01	243.06	4.01
2, 2	266.03	274.75	3.27	276.37	3.89	276.88	4.08
2, 3	381.41	388.3	1.81	392.62	2.94	389.59	2.15
1, 4	420.68	419.56	−0.27	424.03	0.8	420.16	−0.13

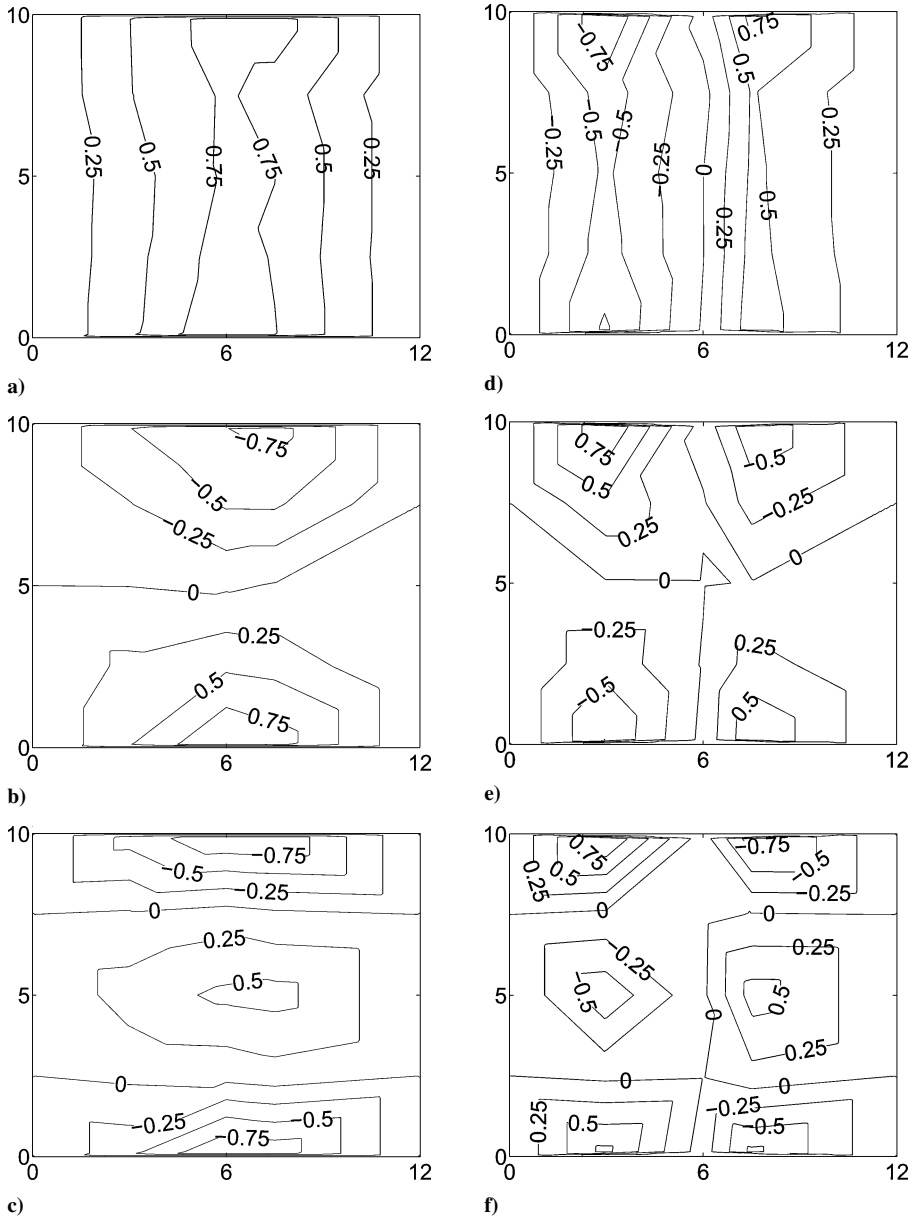

Fig. 5 Contour plot of experimental bending mode shape functions for an aluminum plate with CFCF boundary conditions.

seventh mode. Both analyses tended to overpredict modal frequency, which was expected. As the number of plate modes (derived from beam modes) is increased, the natural frequency prediction error decreases, as shown in Table 4.

The experimental mode shape functions were extracted using the Star software. The mode shape functions are represented by the magnitude and phase at each spanwise location because of damping in the plate. The real components of the mode shapes were used in our analyses. We can reconstruct the mode shape functions for the entire plate using two-dimensional interpolation based on information from these 15 points. The first six mode shape functions are plotted in contour form, as shown in Fig. 5 (parts a–f). From the figure, we can identify the nodal line and mode number clearly. The analytical mode shape functions predicted by the assumed modes method using plate modes are presented as well in Fig. 6 (parts a–f). We noted that the nodal lines in the experimental results were curved, whereas those predicted by analysis are straight lines. Finally we compared the frequency response functions predicted by both analyses at one location on the plate, number 15, as shown in Fig. 7; the coordinates are listed in Table 3. The frequency response functions are plotted in Fig. 8. Both analyses captured the trend of the frequency response functions.

Computational Cost

As shown in Table 4, the first seven plate bending natural frequencies were validated using experimental data. In analysis 1, we included 25 plate modes, each of which were approximated as a product of two beam modes in the x and y directions. In analysis 2, only seven plate modes were used. Both analyses yielded comparable accuracy in frequency predictions. The total computational cost is composed of two parts. The first part involves preparation of the plate mode shape functions and the second part involves matrix eigenvalue calculations after the assumed modes method is applied. In analysis 1, there is no cost to prepare the assumed plate modes because beam mode shape functions are used and available the literature. In analysis 2, we need to predetermine the plate mode shape functions based on the extended Kantorovich–Krylov method. We calculated the first 16 plate mode shape functions for our CFCF plate with an aspect ratio of 1.2. The results are listed in Tables 1 and 2. The code is written in MATLAB. The average number of floating point operations was 250,370. Using a DELL Latitude C-600 notebook with 850 MHz CPU speed, the average CPU time for each mode was 7.04 s. Thus, the computational cost of complete two-dimensional plate modes is insignificant. Also, results can be tabulated for future use

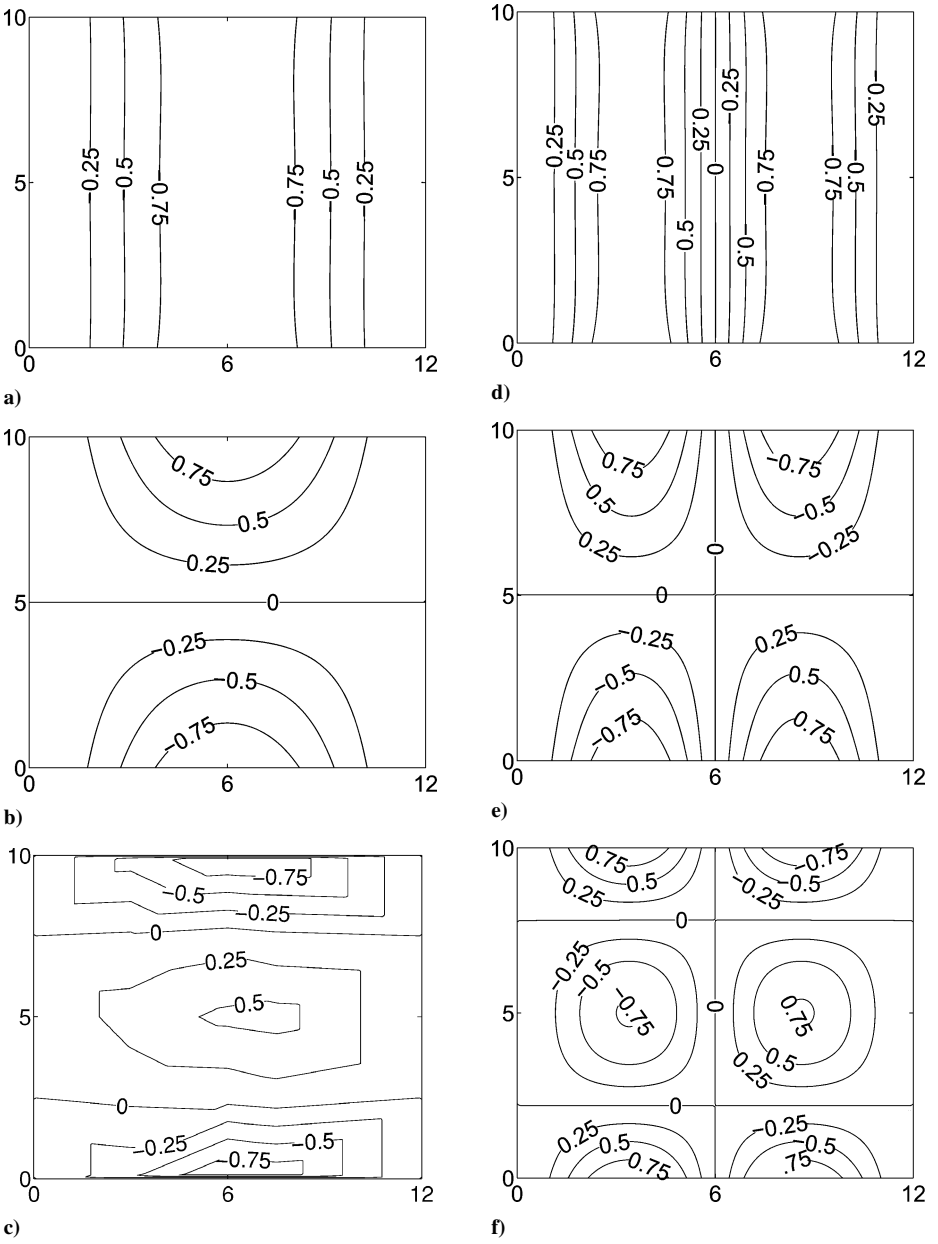

Fig. 6 Contour plot of analytical bending mode shape functions for an aluminum plate with CFCF boundary conditions.

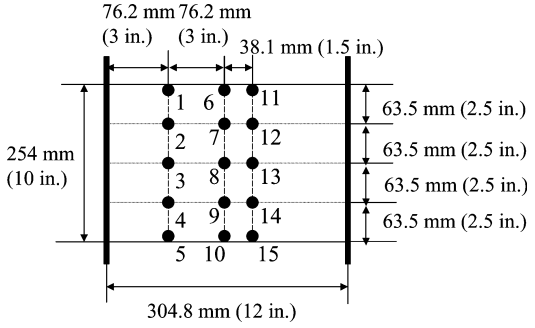

Fig. 7 Schematic of sensor array for plate testing.

as long as the plate boundary conditions and aspect ratio remain the same.

Calculation of the eigenvalues of a symmetric matrix requires $\frac{4}{3}n^3 + \mathcal{O}(n^2)$ operations,[20] where n is the dimension of the matrix. In our analyses, the matrix size was 25×25 in analysis 1 and 7×7 in analysis 2. Therefore, eigenvalue calculation in analysis 2 is about 46 times faster than that in analysis 1. Thus, the use of fewer two-dimensional plate modes

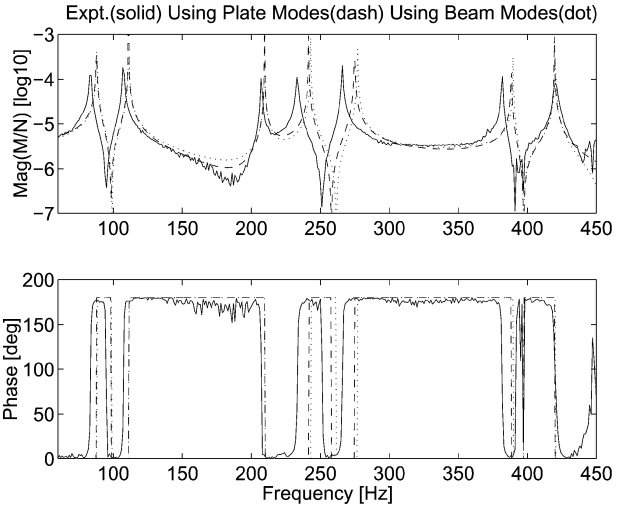

Fig. 8 Frequency response functions of an aluminum plate with CFCF boundary conditions, at location 15, as shown as Table 3; only 7 plate modes were included and 25 beam bending modes were used.

substantially improves computational cost when computing eigenfrequencies.

Our goal is to achieve accurate frequency predictions for plate bending vibration. In analysis 2, we do spend some time to prepare updated plate mode shape functions. However, we need to deal with a relatively small matrix eigenvalue problem later and the frequency predictions are accurate. Overall, the computational cost is an insubstantial factor in analysis 2, although we need to predetermine the plate mode shape functions based on the Kantorovich–Krylov method. Eventually we can achieve better frequency predictions using fewer plate modes in the assumed modes method.

Conclusions

The assumed modes method was used to analyze plate bending vibration. Two analyses were developed. In analysis 1, the plate transverse displacement mode shape functions were approximated by the product of one-dimensional beam mode shapes in both x and y directions. In analysis 2, the plate mode shape functions were determined using the extended Kantorovich–Krylov method and the first seven plate modes were included in our calculations. In analysis 1, a total of 7 or 25 modes were included. Natural frequencies, mode shape functions, and frequency response functions were calculated and validated via experimental data for a rectangular plate with CFCF boundary conditions.

As shown in Table 4, we calculated the first seven plate bending modal frequencies and compared them to experimental results. Using analysis 2, seven plate modes were computed using the extended Kantorovich–Krylov method and were then utilized in an assumed modes method. On the other hand, a total 7 or 25 plate modes, approximated as the product of beam mode shapes, were used in analysis 1. These two-dimensional plate mode shape functions not only substantially reduced the computational cost but also improved our prediction accuracy. The maximum error occurred in the first mode in all analyses, which is usually due to the boundary condition effects. From the second to seventh modes, the maximum error in analysis 2 was 3.37%, whereas the maximum error in analysis 1 was 4.01 and 4.08% when using 7 or 25 plate modes derived from beam modes, respectively. The prediction error in analysis 1 can be reduced by increasing the number of modes in the analysis. However, to obtain natural frequency predictions comparable in accuracy to those of analysis 2, 25 modes must be included in analysis 1, as shown in Table 4.

As shown in Fig. 5, the experimental mode shape functions were plotted in contour form for the first six modes. We can easily identify the nodal lines from the contour plots and then determine the mode number. These mode shape functions were obtained based on the measured displacements at the 15 points as shown in Table 3. The accuracy can be improved by using more sample points or a scanning laser vibrometer. The analytical mode shape functions were plotted as well in Fig. 6 using plate modes. The nodal lines agree with experimental results. In our calculation, we assumed only a single separable term in the plate mode shape functions in the extended Kantorovich–Krylov method. Therefore, the nodal lines are always parallel to the plate edges. To remedy this, we must include more separable terms in the plate mode shape functions to predict nodal lines that are not parallel to the plate edges. This would be particularly important to a plate analysis for all edges free.

As shown in Fig. 8, the frequency responses were plotted and compared to the experimental results. Both analyses capture the trend and shift to slightly higher frequency due to overestimated natural frequency, in which only 7 plate modes were used compared to a total of 25 degrees of freedom when using beam modes.

We assessed the computational cost of analyses 1 and 2. We used MATLAB and a Dell Latitude C-600 notebook with 850 MHz CPU speed. Each of the first seven modes requires an average 7 s of CPU time to complete the extended Kantorovich–Krylov iteration. This amount of CPU time is not a burden with today's computers. The use of two-dimensional plate modes instead of plate modes based on one-dimensional beam modes realized a reduction in computational expense by a factor of 46 with comparable accuracy in the eigenfrequency calculations.

Acknowledgment

Research was supported at the University of Maryland by the U.S. Army Research Office under the FY96 Multidisciplinary University Research Initiative (MURI) in Active Control of Rotorcraft Vibration and Acoustics (Gary Anderson and Tom Doligalski, technical monitors). Lab equipment support was provided to N. M. Wereley under the FY96 Defense University Research Instrumentation Program contract DAAH-0496-10301 (Gary Anderson, technical monitor). D.-C. Chang is supported in part by NSF grant DMS9622249 and a William Fulbright Research Grant.

References

[1]Leissa, A., "Vibration of Plates," NASA SP-160, 1969.

[2]Gorman, D. J., *Vibration Analysis of Plates by the Superposition Method*, World Scentific, River Edge, NJ, 1999.

[3]Leung, A. Y. T., *Dynamic Stiffness and Substructures*, Springer-Verlag, London, 1993.

[4]Blevin, R. D., *Formulas for Natural Frequency and Mode Shape*, Van Nostrand Reinhold, New York, 1979.

[5]Kantorovich, L. V., and Krylov, V. I., *Appproximate Methods of Higher Analysis*, Noordhoff, Groningen, The Netherlands, 1964.

[6]Kerr, A. D., "An Extension of the Kantorovich Method," *Quarterly of Applied Mathematics*, Vol. 26, No. 2, 1968, pp. 219–229.

[7]Kerr, A. D., and Alexander, H., "An Application of the Extended Kantorovich Method to the Stress Analysis of a Clamped Rectangular Plate," *Acta Mechanica*, Vol. 6, No. 1–2, 1968, pp. 180–196.

[8]Kerr, A. D., "An Extented Kantorovich Method for the Solution of Eigenvalue Problems," *International Journal of Solids and Structures*, Vol. 5, No. 6, 1969, pp. 559–572.

[9]Cortinez, V. H., and Laura, P. A. A., "Analysis of Vibrating Rectangular Plates of Discontinuously Varying Thickness by Means of the Kantorovich Extended Method," *Journal of Sound and Vibration*, Vol. 137, No. 3, 1990, pp. 457–461.

[10]Bhat, R. B., Singh, J., and Mundkur, G., "Plate Characteristic Functions and Natural Frequencies of Vibration of Plates by Iterative Reduction of Partial Differential Equation," *Journal of Vibration and Acoustics*, Vol. 115, No. 4, 1993, pp. 177–181.

[11]Rajalingham, C., Bhat, R. B., and Xistris, G. D., "Vibration of Rectangular Plates Using Plate Characteristic Functions as Shape Functions in the Rayleigh-Ritz Method," *Journal of Sound and Vibration*, Vol. 193, No. 2, 1996, pp. 497–509.

[12]Rajalingham, C., Bhat, R. B., and Xistris, G. D., "Closed Form Approximation of Vibration Modes of Rectangular Cantilevered Plates by the Variational Reduced Method," *Journal of Sound and Vibration*, Vol. 197, No. 3, 1996, pp. 263–281.

[13]Wang, G., and Wereley, N. M., "Free In-Plane Vibration of Rectangular Plates," *AIAA Journal*, Vol. 40, No. 5, 2002, pp. 953–959.

[14]Chang, D. C., Wang, G., and Wereley, N. M., "A Generalized Kantorovich Method and Its Application to Free In-Plane Plate Vibration Problem," *Applicable Analysis*, Vol. 80, No. 3, 2002, pp. 493–523.

[15]Chang, D. C., Wang, G., and Wereley, N. M., "Analysis and Application of Extended Kantorovich–Krylov Method," *Applicable Analysis*, Vol. 82, No. 7, 2003, pp. 713–740.

[16]Doyle, J. F., *Wave Propagation in Structures*, 2nd ed., Springer-Verlag, New York, 1997, Chap. 6.

[17]Inman, D. J., *Engineering Vibration*, Prentice–Hall, Englewood Cliffs, NJ, 1994.

[18]Fowler, L., Buchner, S., and Ryaboy, V., "Self-Contained Active Damping System for Pnueumatic Isolation Table," Society of Photo-Optical Instrumentation Engineers, Paper 3991-33, March 2000.

[19]*The STAR System Manuals, Reference Manual 3405-0114*, Spectral Dynamics, San Jose, CA, Nov. 1994.

[20]Isaacson, E., and Keller, H. B., *Analysis of Numerical Methods*, Dover, New York, 1994, Chap. 4.